

Rat as an animal model for studying glutaredoxin-5 gene

Ateeq Ashraf, Najeeb Ullah and Ghayyur Ahmad*

Department of Human Genetics & Molecular Biology, Division of Basic Medical Sciences, University of Health Sciences, Lahore, Pakistan

Abstract: Glutaredoxin-5 (Grx5) is a mitochondrial monothiol, participating in iron-sulfur clusters' biogenesis. It directly maintains normal cytosolic and mitochondrial iron homeostasis, participates in erythropoiesis and oxidative stress sensing, and regulates the oxidative-stress-induced apoptosis. The current investigation involved various techniques to associate rat- and human-Grx5 genes. The rat Grx5 protein's 3D structure was predicted (C-score = \square 1.10) and its stereochemical qualities were validated, with 88.2% of amino-acid-residues in the favoured regions of "Ramachandran plot". Z-score (-5.93) also confirmed reliability of the model. Superimposition results demonstrated 93% resemblance, and COFACTOR server predicted 10 conserved ligand-binding-sites in rat- and human-Grx5. Upstream the ATG start site, 26 conserved and 26 aligned transcription factors' binding sites were identified, indicating resemblances in transcriptional regulation of the gene in two organisms. Rat liver also expressed Grx5, indicating Grx5's possible involvement in hepatic iron metabolism not only in housekeeping but in pathophysiological conditions as well. The investigation concluded that rat could logically be used to study the role of Grx5 during health and disease conditions, understanding of which might prove crucial for targeting Grx5 for managing various acute or chronic iron-induced oxidative stress conditions.

Keywords: Bioinformatics, computational genetics, homology modelling, inflammation, iron, mitochondria.

INTRODUCTION

Iron, one of the key trace metals in the living organisms, is directly or indirectly involved in several vital anabolic and catabolic pathways in health and disease conditions (Huang *et al.*, 2011). During disease conditions particularly, its role becomes even more central due to its ability to donate electron. Iron concentration in plasma normally remains in the range of 10 to 30mM; however, as part of the immune reaction to any injuring noxae, iron is withdrawn from serum and is re-distributed to various vital organs of the body, mainly to the liver where it actively contributes to the inflammatory process (Ganz and Nemeth 2012). Iron re-distribution in the body is with the assistance of various classes of iron regulatory proteins (IRPs) (Ahmad *et al.*, 2011).

Many prosthetic groups such as iron-sulfur (Fe-S) clusters also require iron for their respective functions in the body, and organisms have accordingly developed refined mechanisms to acquire and maintain iron (Rouault 2006). Fe-S clusters are among the earliest and important catalysts in the evolution of biomolecules (Lill and Muhlenhoff 2008). Fe-S proteins in eukaryotes are localized in various components of the cell including the mitochondria, cytosol, endoplasmic reticulum and nucleus, and perform a wide variety of cellular activities, including sensing of iron and oxygen, enzymatic catalysis, DNA replication, DNA repair and regulation of protein translation (Rodriguez-Manzaneque *et al.*, 1999; Wang *et al.*, 2009; Ye *et al.*, 2010).

Glutaredoxin-5 (Grx5), a mitochondrial single-domain monothiol glutaredoxin, is a thiol disulfide oxidoreductase, which directly participates in the mitochondrial and cytosolic iron homeostasis maintenance (Ye *et al.*, 2010). It is required at a stage following the mitochondrial Fe-S clusters' biogenesis (Ye *et al.*, 2010) and facilitates in the Fe-S clusters' transfer to target apoproteins by acting as a scaffold (Berndt *et al.*, 2007; Ye and Rouault 2010). Its deficiency results in low Fe-S clusters biogenesis, causing mitochondrial iron overload and cytosolic iron scarcity that ultimately triggers the IRPs 1 and 2 in the cytosol. During low iron conditions, the IRPs are activated and bind to the 5' end of ferritin mRNA, inhibiting production of ferritin protein; and to the 3' end of TfR mRNA, preventing its degradation by RNases. During high iron concentration in the cytosol the reverse happens, and the IRPs do not bind to 5' end of ferritin mRNA and therefore allowing its translation, while simultaneously facilitating the degradation of TfR mRNA by not binding to its 3' end (fig. 1). The clinical significance of this protein has been shown in studies where a mutation in this gene resulting in its decreased expression caused microcytic sideroblastic anaemia (Camaschella *et al.*, 2007), or where it resulted in hypochromic anaemia due to defective Fe-S cluster assembly which was required for proper haem biosynthesis (Ye *et al.*, 2010). Grx5 acts as an oxidative stress sensor, associated with transcription regulators (Molina-Navarro *et al.*, 2006). In mammalian cells, it not only regulates apoptosis but also is important in protecting cells against oxidative-stress-induced apoptosis (fig. 2) (Linares *et al.*, 2009). During normal

*Corresponding author: e-mail: gahmad@uhs.edu.pk

growth, the Grx5 functions as a housekeeper for the adequate protein-redox-state and also as the mediator that helps to detoxify oxidative damage (Rodriguez-Manzanque *et al.*, 1999). The deficiency of Grx5 protein causes defective Fe-S clusters' biogenesis in various tissues (Ye and Rouault 2010), which affect many components of the cell by generating reactive oxygen species (ROS), ultimately leading to oxidative stress (Linares *et al.*, 2009); for example, Grx5 deficient mitochondria in cardiomyocytes have been reported to participate in the development of cardiovascular diseases due to abrogated iron metabolism in these cells (Kalinina *et al.*, 2008).

Rat is the most common animal being used to study various disease-conditions; however, because of the variations in the structures and regulation patterns of various genes and the corresponding proteins, not all the data generated in this animal model are applicable to human. The present study aimed at predicting the differences and similarities between the rat and the human Grx5 both at gene and at protein levels by developing *in silico* 3D structure of rat Grx5, its validation, establishing its structural features and by developing phylogenetic relationship of rat Grx5 to human Grx5. Differences in gene expression regulation of Grx5 were predicted by comparing the transcription factors' binding sites in the gene promoters of both organisms. Moreover, Grx5 gene expression was analysed in the rat liver through polymerase chain reaction.

MATERIALS AND METHODS

Retrieval of rat Grx5 protein sequence

The aim of current study was to perform structure-based sequence analyses on Grx5 protein of rat. The rat Grx5 amino acid sequence was obtained from NCBI protein database using the accession number NP_001102192.1 to generate the three-dimensional structure of the protein using homology modeling. It was also confirmed the non-availability of crystal or NMR structure of rat Grx5 protein in the PDB.

Calculation of physical parameters

Physical parameters of the rat Grx5 protein were determined to obtain general idea about the subunits. ProtParam (Wilkins *et al.*, 1999) online tool was used to compute different parameters of primary structure that included the molecular weight, theoretical isoelectric point (pI), aliphatic index, amino acid composition, atomic composition, extinction coefficient, estimated half-life, and Grand average of hydropathicity" (GRAVY).

Sequence alignment for conservation analysis

Amino acid sequences of rat Grx5 (accession number NP_001102192.1) and human Grx5 (accession number NP_057501.2) were obtained from the NCBI database and subjected to pairwise sequence alignment using "Needleman-Wunsch algorithm" to find out the conserved

residues making the structural motifs (Needleman and Wunsch 1970).

Phylogenetic analysis of Grx5

The evolutionary relationship between rat and human Grx5 was further confirmed by phylogenetic analysis. The phylogenetic tree of Grx5 was constructed by MAFFT online v7.0. For this purpose, multispecies protein sequences of Grx5 homologues in FASTA format were obtained from eggNOG v3.0 (Muller *et al.*, 2010) and submitted to MAFFT online server v7.0 to construct evolutionary tree (Katoh and Standley 2013).

Secondary structure analysis

Secondary structure of rat Grx5 was predicted by PDBsum server was analyzed through various online servers. System classification and disulfide connectivity of secondary structure was analyzed by DiANNA tool (Ferre and Clote 2005).

Tertiary structure prediction, stereochemical analysis and model evaluation

To generate the rat Grx5 3D protein's structure through homology modeling, the I-TASSER online server (Zhang 2008) was used. The generated 3D model was subjected to structure analysis and stereochemical analysis by various evaluation and validation tools. The PROCHECK server (Laskowski *et al.*, 1993) generated the Psi/Phi Ramachandran plot which is used to evaluate the backbone conformation and also check non-GLY residues at the disallowed regions. Quality of the generated 3D model was assured by Z-score using ProSA web tool (Wiederstein and Sippl 2007) which provides the overall model quality and also give surety about the generated structure that is within the range of score as found in the native protein.

Ligand binding site identification

For the identification of the possible ligand binding sites, COFACTOR server (Roy *et al.*, 2012) predicted the rat Grx5 ligand binding sites using different templates.

Predicted rat Grx5 3D structure alignment with human Grx5

The final predicted Grx5 3D structure of rat was aligned with 3D structure of human Grx5 using DaliLite server. The server made a pairwise comparison between the two proteins. The "heuristic algorithm" was used to illustrate random structural alignments of proteins with different folds (Holm and Park 2000).

Promoter analysis for common transcription factors' binding sites

rVISTA 2.0 online tool (Loots and Ovcharenko 2004) was used to obtain functional transcription factors' binding sites (TFBS) conserved across rat and human. For this purpose, nucleotide sequences of 1000bp upstream to the

Table 1: Template proteins with similar binding site in protein data bank (PDB)

Rank	(a) C-score ^{LB}	PDB Hit	(b) TM-score	(c) RMSD ^a	(d) IDEN ^a	(e) Cov.	(f) BS-score	Lig. Name	Predicted binding site residues
1	0.90	2wulA	0.666	1.37	0.917	0.717	1.97	Mul. Part	55, 63, 65, 93, 97, 104, 105, 117, 118, 119
2	0.53	2yanB	0.644	1.47	0.429	0.691	1.62	GTT	55, 62, 63, 65, 93
3	0.21	3grxA	0.477	1.81	0.220	0.539	1.25	GTT	63, 65, 102, 103, 104, 105
4	0.21	2wciA	0.668	1.62	0.336	0.724	1.75	NA	61, 62, 63, 64, 68

Table 2: ‘TM-align’ computer algorithm showing the proteins with highly similar structures in Protein Data Bank (PDB)

Rank	PDB Hit	(a)TM-score	(b)RMSD ^a	(c)IDEN ^a	(d)Cov.
1	3ipzA	0.701	0.70	0.495	0.717
2	2wulD	0.671	1.30	0.917	0.717
3	2wciA	0.668	1.62	0.336	0.724
4	3gx8A	0.658	1.59	0.477	0.717
5	2yanA	0.643	1.46	0.429	0.691
6	1z7rA	0.634	2.35	0.248	0.717
7	3d4mA	0.631	1.35	0.252	0.678
8	3zywA	0.627	1.47	0.352	0.678
9	3c1rA	0.625	1.51	0.202	0.684
10	2jadA2	0.625	2.07	0.188	0.704

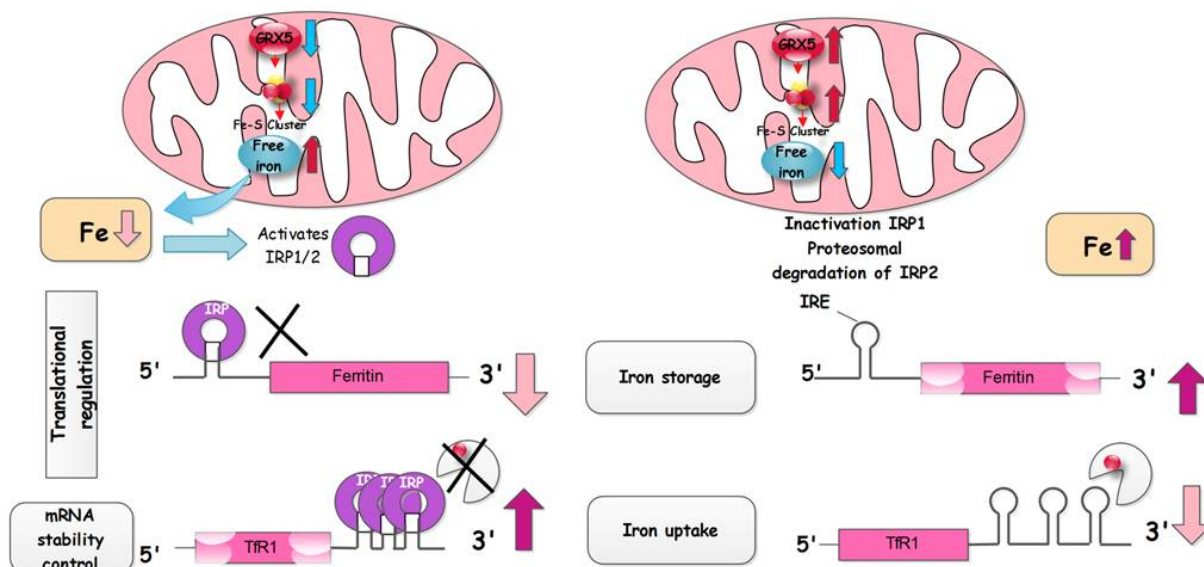


Fig. 1: Grx5 regulates cellular iron homeostasis: Mitochondrial Fe-S clusters biogenesis by Grx5 and its effects on cytosolic IRP1 and IRP2. “↑” and “↓” indicate increase and decrease respectively. (The diagram was drawn using “Edraw Mind Map 6.8” software.)

ATG start site were retrieved from Ensembl database, and submitted in FASTA format to rVISTA v2.0 online server.

Animal dissections

Six weeks old, male Wistar-derived rats were purchased from National Institute of Health, Islamabad, Pakistan. In accordance with the institutional guidelines and the National Institutes of Health’s guidelines, animals were humanely handled, were given standard laboratory chow,

free access to water, and were maintained on a 12h:12h light: dark cycle. The ethical review board of University of Health Sciences, Lahore, Pakistan approved the protocol for experiments on animals. Animals were anaesthetized using ether, and were then sacrificed. The liver was excised, rinsed with physiological saline solution, snap frozen in liquid nitrogen and stored at -80°C until further use.

conservation and evolutionary relationship of Grx5 protein in rat and human.

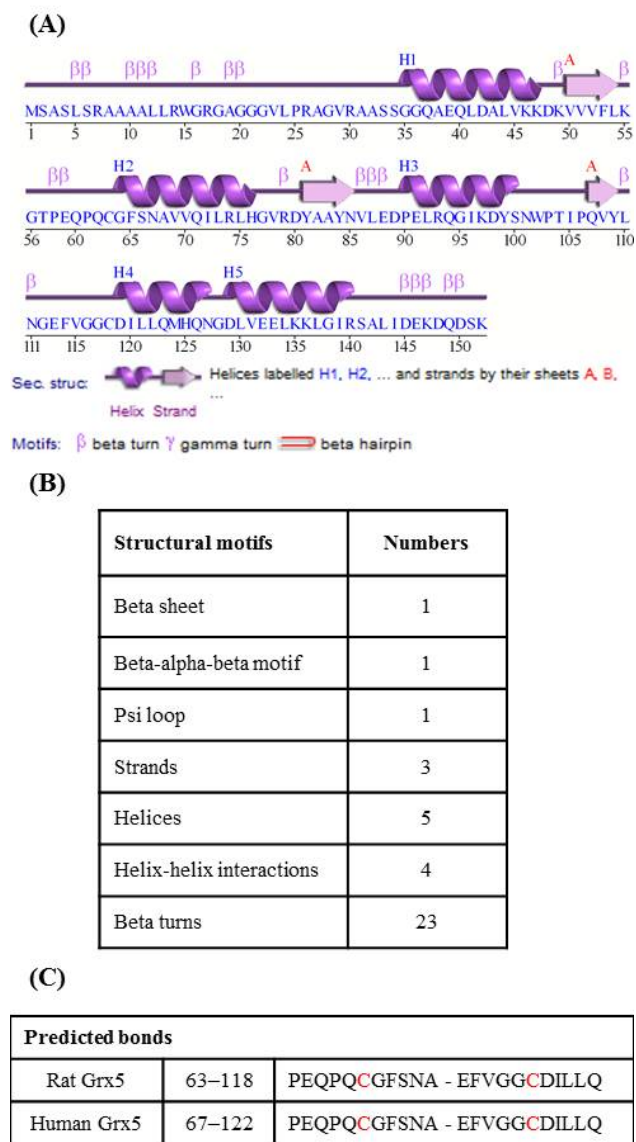


Fig. 4: Secondary structure of rat Grx5 protein: (A) The secondary structural elements. (B) Number of structural motifs observed. (C) Disulfide bonds predicted by DiANNA tool, showing cysteine residues involved in protein fold stabilization.

Secondary structure analysis

PDBsum server analysis revealed the presence of beta turns, beta sheets, beta-alpha-beta motif, psi loop, strands, helices, helix-helix interactions, and coils in Grx5 protein of rat (fig. 4A & 4B). Disulfide bonds were predicted by DiANNA tool (fig.4C) which can be useful in understanding the secondary structure of the protein and the disulfide bond bridges are important in protein fold stabilization. Disulfide connectivity was predicted to be in between 1-2 (between cysteines 63 and 118).

Three dimensional structure prediction and validation

The 3D structure of proteins are important for providing information about protein functions, interactions and localizations (Ferre and Clote 2005). Therefore, I-TASSER online server generated the 3D structures of rat Grx5 and the best predicted-structure having maximum confidence score (C-score = 1.10) was chosen (fig. 5). Ramachandran plot and Z-score evaluated the quality and reliability of the predicted structure. Ramachandran plot checked the stereochemical quality of the 3D structure via analyzing residue by residue geometry and overall structure geometry. The red shaded areas are the "core" regions indicating the most favourable combinations of phi-psi values (fig. 6A). The result showed that 88.2% of residues are present in favourable/core region and 0.8% residues in disallowed regions of the Ramachandran plot (fig. 6B) representing an acceptable stereochemical quality of the predicted model. ProSA tool was used to analyze overall quality of the predicted model. The Z-score value calculated by ProSA tool, for rat Grx5 protein was -5.93 (fig.6C). The results of Ramachandran plot and Z-score confirmed the quality of the homology model of rat Grx5 protein.

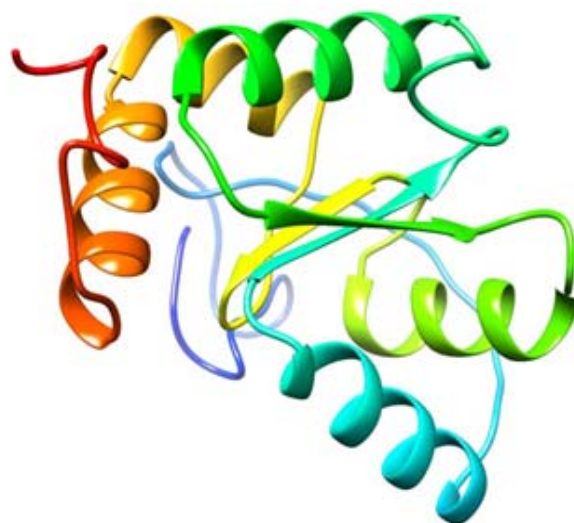
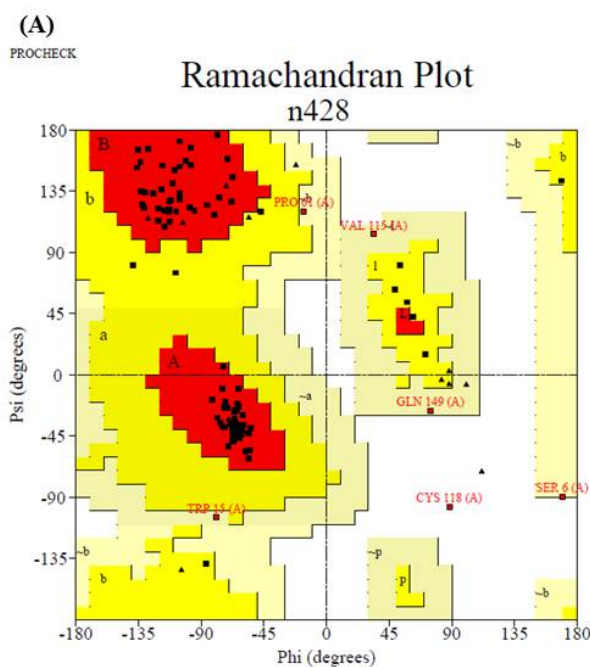


Fig. 5: Three-dimensional (3D) protein structure of rat Grx5: UCSF Chimera visualization tool used to view and analyze rat Grx5 3D structure generated through I-TASSER server.

Predicted ligand binding sites

The identification of binding site by COFACTOR server predicted the following ten binding sites' residues and their positions; Lys55, Cys63, Phe65, Arg93, Lys97, Thr104, Ile105, Gly117, Cys118 and Asp119 that are conserved in human Grx5 on the basis of C-score^{LB}= 0.90, TM-score= 0.666 and RMSD^a= 1.37. Template proteins with similar binding site are also presented in (table 1).



(B)

Ramachandran plot statistics		
Residues in	No. of residues	Percentage
Most favoured regions [A,B,L]	112	88.2%
Additional allowed regions [a,b,l,p]	10	7.9%
Generously allowed regions [~a,~b,~l,~p]	4	3.1%
Disallowed regions	1	0.8%
Number of non-glycine and non-proline residues	127	100.0%
Number of end-residues (excl. Gly and Pro)	2	
Number of glycine residues (shown as triangles)	17	
Number of proline residues	6	
Total number of residues	152	

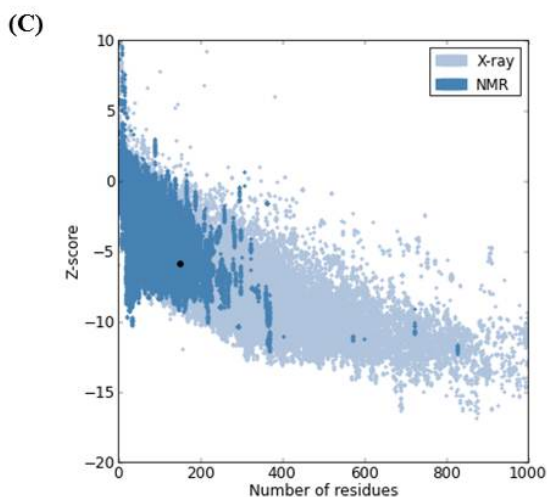
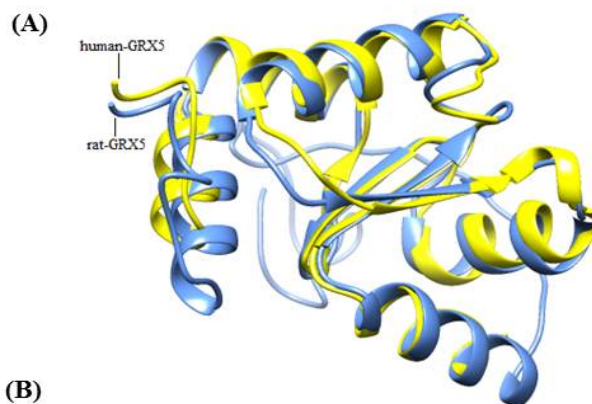


Fig. 6: Model evaluation of rat Grx5: (A) Ramachandran plot showing the stereochemical spatial arrangement of amino acid residues. (B) Ramachandran plot statistics

showing the percentage residues of Grx5 protein. (C) Z-score showing the quality of the 3D structure.

Rat Grx5 3D structures alignment with crystal structure of human Grx5

The rat Grx5 3D protein structure was aligned with crystal structure of human Grx5 through DaliLite server by pairwise comparison of the two proteins' structures simultaneously (fig. 7). The rat Grx5 protein's structure superimposition analysis illustrated 93% resemblance with human Grx5 based on Z-score= 15.6 and RMSD= 1.3.



(B)

Name	Z-score	Number of equivalent residues	Root-mean-square deviation of C-alphas (Angstrom)	Sequence Identity%
Rat+Human (2wulD)	15.6	109	1.3	93

Fig. 7: Superimposition of 3D model of rat Grx5: (A) Superimposition of rat Grx5 on chain D of human Grx5 (PDB ID: 2wulD). (B) Pairwise alignment score between predicted structure of rat Grx5 and crystal Grx5 structure of human.



Fig. 8: Conserved transcription factors across rat and human Grx5 analyzed through rVISTA v2.0 server.

Promoter analysis for common transcription factors' binding sites

Promoter analysis detected 364 TFBS in the base sequence of rat and 439 TFBS detected in the human Grx5 sequence, upstream to the ATG start site. Promoter analysis also identified 26 conserved and 26 aligned TFBS, shown in (fig. 8).

Expression of Grx5 in rat liver

The basal expression analysis of Grx5 gene in rat liver was done through qualitative PCR analysis, which showed that Grx5 was expressed in rat liver tissue in housekeeping conditions (fig. 9A) and therefore could be involved in regulating iron metabolism and related basal housekeeping functions. Hecpudin and β -actin were used as positive control genes (fig. 9B & 9C) to validate the PCR. Two types of negative controls i.e., one without cDNA and one without primer pair for all primer pairs were used to further confirm that the PCR reaction only amplified the desired gene products and that no unwanted non-specific PCR product was amplified under the given thermal cycling conditions.

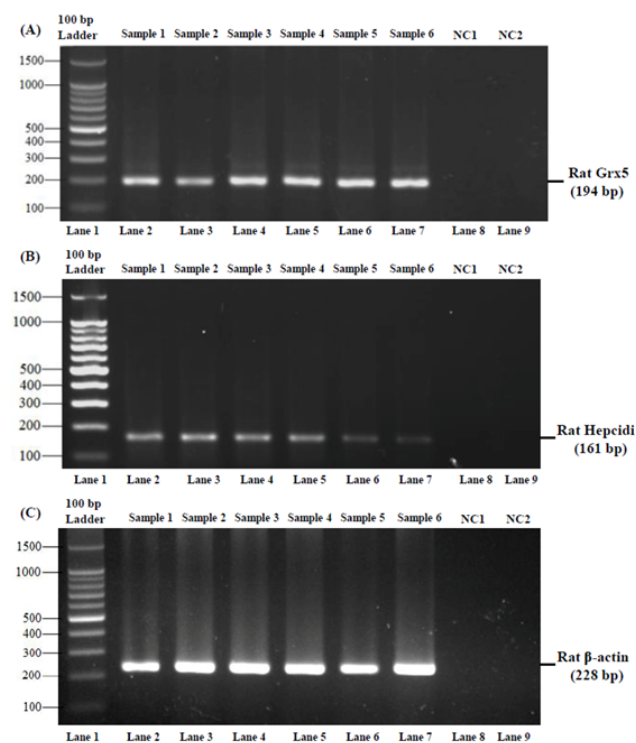


Fig. 9: Basal expression of Grx5, hepcidin and β -actin genes in rat liver: NC1 and NC2 are the negative controls of primers and cDNA respectively. (A) Amplicons of Grx5 gene (194 bp). (B) Amplicons of hepcidin gene (161 bp). (C) Amplicons of β -actin gene (228 bp).

DISCUSSION

Computational genetic approaches have a great many roles not only in the prediction but also in the

confirmation of established laboratory-based investigations in the *de novo* analysis. During the course of current investigation, various computational genetic tools were used to analyze the similarities between rat and human Grx5 proteins. Physical characteristics of the protein, accessed computationally and through sequence alignment showed highly conserved regions of rat and human Grx5. Mammals and other vertebrates have a conserved Grx5 region "CGFS" where Fe-S cluster bridges two subunits as a ligand along with two GSH molecules. Many other conserved residues are also considered to be occupied where GSH ligand docks to the Grx5 protein (Ye *et al.*, 2010). Our approach showed that both the rat's and the human's Grx5 proteins had this conserved region "CGFS". Phylogenetic analysis further confirmed the evolutionary relationship of Grx5 protein (fig. 3).

In protein-folding prediction, the positions of disulfide bridges are important in finding out the conformational space. Therefore the correct prediction of the disulfide connectivity helps in prediction of the 3D structure of a protein (Fariselli and Casadio 2001). Rat Grx5 protein has two cysteines that form a disulfide bond, with connectivity pattern 1-2 (between cysteines 63 and 118) (fig.4C). Disulfide bonds are formed by covalent attachment of sulfur atoms from cysteine residues, and involved in protein structure stabilization (Ferre and Clote 2005). In addition to cysteine 63 in rat Grx5 sequence and cysteine 67 in human Grx5 sequence at the "CGFS" site, both Grx5 sequences have a second cysteine (Cys 118 in rat Grx5 and Cys 122 in human Grx5) which is conserved. Wang and colleagues have shown that this second cysteine residue may be involved in the antioxidant activity of Grx5 (Wang *et al.*, 2009).

PDBsum server was used to analyze the rat Grx5 secondary structural motif. The secondary structure showed the presence of 1 beta sheet, 1 beta-alpha-beta motif, 1 psi loop, 3 strands, 5 helices, 4 helix-helix interactions and 23 beta turns (fig. 4B). Secondary structure elements and motifs are arranged in different combinations to form domains. A polypeptide chain is thus a sequential arrangement motif.

The three-dimensional structures can be helpful in the identification of rat Grx5 protein's structure, function and putative active site residues. Moreover, the predicted 3D structure can not only be helpful in drug designing but also in understanding the interactions between proteins (Vyas *et al.*, 2012). Therefore, I-TASSER online server was used to predict the 3D structure of the rat Grx5 protein. Based on the maximum confidence score and maximum number of decoys, the most suitable Grx5 3D structure was chosen for evaluation and verifications. Confidence score (C-score) assessed the quality of proteins' models, predicted by I-TASSER. The C-score value ranges from -5 to 2 and a higher value of C-score

means a model with a high confidence and vice-versa (Zhang 2008). The predicted model of the rat Grx5 has the C-score of -1.10, and Maximum number of decoys = 5830, TM-score = 0.58 ± 0.14 and RMSD = $7.1 \pm 4.2 \text{ \AA}$.

The template modeling score (TM-score) was used to assess the structural resemblance between model and templates (Zhang and Skolnick 2004). The sequence identity in the structurally aligned regions was also determined. I-TASSER server predicted ten structure-models of rat Grx5 protein. The selected model and the templates showed the structural similarity which had expected TM-score ranging from 0.701 to 0.625 and RMSD (root mean square deviation) score lied between 0.70 and 2.07 \AA for Grx5 proteins from I-TASSER server (table 2). The results of C-score, TM-score and RMSD suggested the selected models in correct topology.

Ramachandran plot of protein backbone torsions phi/psi (Φ/Ψ) are used to authenticate the 3D structures of proteins (Frank *et al.*, 2007). It plots the complete conformational space of a polypeptide and explains the allowed and disallowed conformations (Sun *et al.*, 2012). The topology of the protein 3D structure is actually under the control of three backbone dihedral torsion angles along with the protein peptide chains, i.e. ϕ (involving backbone atoms C-N-C α -C), ψ (N-C α -C-N), and ω (C α -C-N-C α). However, the torsion angle ω is almost fixed at 180° with rare *cis* cases of 0° due to the planarity of the partial-double peptide bond. So with known values of phi (ϕ) and psi (ψ) angles, the overall geometry of the protein structures can be built (Wu and Zhang 2008). The stereochemical qualities of the predicted rat Grx5's 3D model were verified by Ramachandran plot using PROCHECK server, which explained the phi-psi torsion angles for all residues in the structure (apart from the chain termini location). The results signified that the 88.2% residues were present in the allowed/core region, 7.9% of residues were in additional allowed regions and 0.8% of residues has phi-psi angles in the disallowed regions (fig. 6B), signifying the suitability of the Ramachandran plot and a satisfactory stereochemical quality of the rat Grx5 protein model.

ProSA tool was also used to evaluate three dimensional model of rat Grx5 protein for potential errors (Wiederstein and Sippl 2007). It calculated the Z-score value to describe model quality and measured the energy efficiency of the structure. The Z-scores values outside a specified range for native proteins designate incorrect structures (Wiederstein and Sippl 2007). The Z-score value of minus 5.93 for rat Grx5 protein confirmed the reliability of the model (fig. 6C).

To determine homology between two or more structures, structural alignment is performed on the basis of their shape and 3D conformation (Hung and Lin 2013). It can also be used on protein tertiary structures and for large

RNA molecules. The rat Grx5 3D structure alignment with human Grx5 showed Z-score 15.6, root-mean-square deviation (RMSD) of C-alphas (Angstrom) value 1.3 and 93% resemblance with human Grx5 3D structure (PDB ID: 2wu1D). The similarity is based on the shape and three-dimensional conformation between rat and human Grx5 3D structures.

Ligand binding site is usually the largest cleft in a protein and is the region where the protein interacts with a specific molecule or ion. Proteins are usually ligand specific and the identification and comparison of such regions in a protein can suggest putative functions (Loewenstein *et al.*, 2009). In protein-ligand binding, ligand is generally a signal-triggering molecule that binds to a location in the target protein, commonly in the largest cleft of the protein. When a ligand binds to a receptor protein, it alters its conformation, which establishes its functional state. The COFACTOR server selected the template protein with similar binding sites on the basis of C-score^{LB}, which is the confidence score of predicted binding site. The value of C-score^{LB} ranges from 0 to 1; and a more reliable ligand-binding site prediction is confirmed by higher score (Roy *et al.*, 2012). COFACTOR server predicted 10 conserved binding sites' residues at positions Lys55, Cys63, Phe65, Arg93, Lys97, Thr104, Ile105, Gly117, Cys118 and Asp119 with that of human Grx5 protein structure (PDB ID: 2wu1A), (C-score^{LB} = 0.90) (table 1). Upstream the ATG start site, the promoter analysis identified 26 conserved and 26 aligned transcription factors' binding sites (TFBS), indicating resemblances in transcriptional regulation of the gene in the two organisms.

Major changes in iron metabolism take place during various pathological conditions and liver is the main organ regulating iron homeostasis of the body (Anderson and Shah 2013).

CONCLUSION

The current study is the first to show that Grx5, an iron regulatory protein, is expressed in normal housekeeping conditions in rat liver. This basal expression not only indicates that Grx5 is involved in hepatic iron regulation during various physiological conditions but also points towards its participation in iron-induced oxidative stress during pathological conditions as well. The results of the computational analysis logically suggest that rat can be used as an animal model of choice to study the role of Grx5 in iron regulation during health and disease conditions.

ACKNOWLEDGEMENTS

University of Health Sciences, Lahore, Pakistan supported this project from its indigenous research funding.

REFERENCES

- Ahmad G, Sial GZ, Ramadori P, Dudas J, Batusic DS and Ramadori G (2011). Changes of hepatic lactoferrin gene expression in two mouse models of the acute phase reaction. *Int. J. Biochem. Cell Biol.*, **43**: 1822-1832.
- Anderson ER and Shah YM (2013). Iron homeostasis in the liver. *Compr. Physiol.*, **3**: 315-330.
- Berndt C, Lillig CH and Holmgren A (2007). Thiol-based mechanisms of the thioredoxin and glutaredoxin systems: implications for diseases in the cardiovascular system. *Am. J. Physiol Heart Circ. Physiol.*, **292**: H1227-H1236.
- Camaschella C, Campanella A, De FL, Boschetto L, Merlini R, Silvestri L, Levi S and Iolascon A (2007). The human counterpart of zebrafish shiraz shows sideroblastic-like microcytic anemia and iron overload. *Blood*, **110**: 1353-1358.
- Fariselli P and Casadio R (2001). Prediction of disulfide connectivity in proteins. *Bioinformatics.*, **17**: 957-964.
- Ferre F and Clote P (2005). DiANNA: A web server for disulfide connectivity prediction. *Nucleic Acids Res.*, **33**: W230-W232.
- Frank M, Lutteke T and von der Lieth CW (2007). GlycoMapsDB: A database of the accessible conformational space of glycosidic linkages. *Nucleic Acids Res.*, **35**: 287-290.
- Ganz T and Nemeth E (2012). Iron metabolism: interactions with normal and disordered erythropoiesis. *Cold Spring Harb. Perspect. Med.*, **2**: a011668.
- Holm L and Park J (2000). DaliLite workbench for protein structure comparison. *Bioinformatics.*, **16**: 566-567.
- Huang ML, Lane DJ and Richardson DR (2011). Mitochondrial mayhem: The mitochondrion as a modulator of iron metabolism and its role in disease. *Antioxid. Redox. Signal.*, **15**: 3003-3019.
- Hung CL and Lin YL (2013). Implementation of a parallel protein structure alignment service on cloud. *Int. J. Genomics*, **2013**: 439681.
- Kalinina EV, Chernov NN and Saprin AN (2008). Involvement of thio-, peroxi- and glutaredoxins in cellular redox-dependent processes. *Biochemistry (Mosc.)*, **73**: 1493-1510.
- Katoh K and Standley DM (2013). MAFFT multiple sequence alignment software version 7: Improvements in performance and usability. *Mol. Biol. Evol.*, **30**: 772-780.
- Laskowski RA, Moss DS and Thornton JM (1993). Main-chain bond lengths and bond angles in protein structures. *J. Mol. Biol.*, **231**: 1049-1067.
- Lill R and Muhlenhoff U (2008). Maturation of iron-sulfur proteins in eukaryotes: mechanisms, connected processes, and diseases. *Annu. Rev. Biochem.*, **77**: 669-700.
- Linares GR, Xing W, Govoni KE, Chen ST and Mohan S (2009). Glutaredoxin 5 regulates osteoblast apoptosis by protecting against oxidative stress. *Bone*, **44**: 795-804.
- Loewenstein Y, Raimondo D, Redfern OC, Watson J, Frishman D, Linial M, Orengo C, Thornton J and Tramontano A (2009). Protein function annotation by homology-based inference. *Genome Biol.*, **10**: 207.
- Loots GG and Ovcharenko I (2004). rVISTA 2.0: Evolutionary analysis of transcription factor binding sites. *Nucleic Acids Res.*, **32**: W217-W221.
- Molina-Navarro MM, Casas C, Piedrafita L, Belli G and Herrero E (2006). Prokaryotic and eukaryotic monothiol glutaredoxins are able to perform the functions of Grx5 in the biogenesis of Fe/S clusters in yeast mitochondria. *FEBS Lett.*, **580**: 2273-2280.
- Muller J, Szklarczyk D, Julien P, Letunic I, Roth A, Kuhn M, Powell S, von MC, Doerks T, Jensen LJ and Bork P (2010). eggNOG v2.0: Extending the evolutionary genealogy of genes with enhanced non-supervised orthologous groups, species and functional annotations. *Nucleic Acids Res.*, **38**: D190-D195.
- Needleman SB and Wunsch CD (1970). A general method applicable to the search for similarities in the amino acid sequence of two proteins. *J. Mol. Biol.*, **48**: 443-453.
- Rodriguez-Manzaneque MT, Ros J, Cabisco E, Sorribas A and Herrero E (1999). Grx5 glutaredoxin plays a central role in protection against protein oxidative damage in *Saccharomyces cerevisiae*. *Mol. Cell Biol.*, **19**: 8180-8190.
- Rouault TA (2006). The role of iron regulatory proteins in mammalian iron homeostasis and disease. *Nat. Chem. Biol.*, **2**: 406-414.
- Roy A, Yang J and Zhang Y (2012). COFACTOR: An accurate comparative algorithm for structure-based protein function annotation. *Nucleic Acids Res.*, **40**: W471-W477.
- Sun J, Tang S, Xiong W, Cong P, and Li T (2012). DSP: A protein shape string and its profile prediction server. *Nucleic Acids Res.*, **40**: W298-W302.
- Vyas VK, Ukawala RD, Ghate M and Chintha C (2012). Homology modeling a fast tool for drug discovery: current perspectives. *Indian J. Pharm. Sci.*, **74**: 1-17.
- Wang Y, He YX, Yu J and Zhou CZ (2009). Cloning, overproduction, purification, crystallization and preliminary X-ray diffraction analysis of yeast glutaredoxin Grx5. *Acta Crystallogr. Sect. F. Struct. Biol. Cryst. Commun.*, **65**: 651-653.
- Wiederstein M and Sippl MJ (2007). ProSA-web: interactive web service for the recognition of errors in three-dimensional structures of proteins. *Nucleic Acids Res.*, **35**: W407-W410.
- Wilkins MR, Gasteiger E, Bairoch A, Sanchez JC, Williams KL, Appel RD and Hochstrasser DF (1999). Protein identification and analysis tools in the ExPASy server. *Methods Mol. Biol.*, **112**: 531-552.

- Wu S and Zhang Y (2008). ANGLOR: A composite machine-learning algorithm for protein backbone torsion angle prediction. *PLoS. One.*, **3**: e3400.
- Ye H, Jeong SY, Ghosh MC, Kovtunovych G, Silvestri L, Ortillo D, Uchida N, Tisdale J, Camaschella C and Rouault TA (2010). Glutaredoxin 5 deficiency causes sideroblastic anemia by specifically impairing heme biosynthesis and depleting cytosolic iron in human erythroblasts. *J. Clin. Invest.*, **120**: 1749-1761.
- Ye H and Rouault TA (2010). Human iron-sulfur cluster assembly, cellular iron homeostasis and disease. *Biochemistry*, **49**: 4945-4956.
- Zhang Y (2008). I-TASSER server for protein 3D structure prediction. *BMC Bioinformatics.*, **9**: 40.
- Zhang Y and Skolnick J (2004). Scoring function for automated assessment of protein structure template quality. *Proteins*, **57**: 702-710.